

RESEARCH ARTICLE

Antibiotics confound breath-based respiratory disease detection in calves

Ben Langford^{1*}, Johanna Brans², Claire Broadbent², Tim Gibson³, Mark Hanlon¹, Marie Haskell², Laura Nicoll², Neil J. Mullinger¹, Carol-Anne Duthie²

1 UK Centre for Ecology and Hydrology, Bush Estate, Penicuik, United Kingdom, **2** SRUC, Edinburgh, United Kingdom, **3** RoboScientific Ltd, Espace North, Littleport, Cambridgeshire, United Kingdom

* benngf@ceh.ac.uk



Abstract

Breath analysis offers a promising, non-invasive approach for early disease detection in livestock, particularly for bovine respiratory disease (BRD). However, the widespread use of antibiotics in veterinary practice raises concerns about their potential to confound breath-based diagnostics. In this study, we analysed breath samples from 65 calves to evaluate the diagnostic performance of volatile organic compounds (VOCs) as biomarkers of BRD. We identified several candidate ions, including formaldehyde and acetone/propanal, that showed significant elevation at the onset of disease and a modest detection capability (AUC=0.53-0.77). However, the strongest discrimination between diseased and controls occurred after antibiotic administration, suggesting a confounding pharmacological influence. To isolate this effect, a secondary trial was conducted in which healthy calves were treated with oxytetracycline dihydrate (Alamycin® LA 300). This revealed rapid and transient changes in the breath volatilome, with significant increases in dimethyl sulphide and (C₅H₁₀O)H⁺ within 1 hour, and other VOCs, including formaldehyde and acetone/propanal within 24 hours of treatment. These findings demonstrate that antibiotics can substantially alter breath VOC profiles, potentially mimicking or masking disease signals. We conclude that breath-based diagnosis of BRD holds promise but must account for treatment history to avoid misclassification. Moreover, the reproducible and time-resolved nature of the VOC response suggests that breath analysis could also be developed as a tool for monitoring antimicrobial exposure and optimising therapeutic dosing in livestock.

OPEN ACCESS

Citation: Langford B, Brans J, Broadbent C, Gibson T, Hanlon M, Haskell M, et al. (2026) Antibiotics confound breath-based respiratory disease detection in calves. *PLoS One* 21(6): e0351838. <https://doi.org/10.1371/journal.pone.0351838>

Editor: Angel Abuelo, Michigan State University, UNITED STATES OF AMERICA

Received: December 17, 2025

Accepted: June 2, 2026

Published: June 24, 2026

Peer Review History: PLOS recognizes the benefits of transparency in the peer review process; therefore, we enable the publication of all of the content of peer review and author responses alongside final, published articles. The editorial history of this article is available here: <https://doi.org/10.1371/journal.pone.0351838>

Copyright: © 2026 Langford et al. This is an open access article distributed under the terms of the [Creative Commons Attribution License](https://creativecommons.org/licenses/by/4.0/), which permits unrestricted use, distribution,

1. Introduction

Breath analysis has emerged as a powerful tool for non-invasive disease detection in human healthcare, offering real-time diagnostic insights through the analysis of volatile organic compounds (VOCs) [1–3]. The technique has been applied to a range of clinical challenges for humans, including the detection of metabolic disorders

and reproduction in any medium, provided the original author and source are credited.

Data availability statement: All breath measurements are available from the Zenodo database (<https://zenodo.org/records/17940806> DOI: 10.5281/zenodo.17940805).

Funding: This work was funded as part of the Innovate UK grant (Project # 10072590): DETECT. The funders had no role in study design, data collection and analysis, decision to publish, or preparation of the manuscript.

Competing interests: The authors have declared that no competing interests exist.

[4], cancer biomarkers [5], and infectious diseases [3], owing to its ability to reflect systemic physiological changes without the need for invasive sampling [1–3]. More recently, breathomics has begun gaining traction in animal health research, with growing interest in its application to veterinary medicine [6,7]. Early studies have demonstrated its potential for identifying paratuberculosis [8], monitoring ketosis in dairy cows [9,10], and even detecting pregnancy through VOC profiling [11]. Recent reviews continue to highlight the rapid progress in breathomics and its expanding diagnostic potential in both human and veterinary medicine, including advances in GC-MS and PTR-MS breath profiling, electronic-nose technologies and nanosensors [12–15]. These developments underline the growing feasibility of using exhaled VOCs for early disease detection and real-time monitoring across a wide range of pathological conditions.

Given its promise, breath-based diagnostics could play a transformative role in the detection of bovine respiratory disease (BRD), one of the most economically significant illnesses affecting cattle worldwide [16]. BRD is a complex syndrome, initiated by viral infections that predispose young calves to secondary bacterial invasion, leading to pneumonia and impaired respiratory function [17,18]. With calf pneumonia affecting 20–30% of herds in the UK [17], the economic and welfare implications are substantial [19] and include reduced growth rates, increased veterinary costs [20], and elevated mortality risk in pre-weaned calves [20–23]. Traditional diagnostic approaches rely on visual observation of symptoms, yet these signs are often non-specific, leading to delayed intervention. Breath analysis offers an alternative: a metabolic fingerprint capable of detecting physiological changes linked to disease onset, with some studies showing early promise [7,24–28]. Moreover, a new generation of low-cost VOC sensors is emerging, offering the potential for on-farm diagnostic tools, that can be incorporated into existing infrastructure such as close to feeders and water troughs that animals visit several times a day. However, it must be ensured that reliable and disease-specific breath signatures can be identified and that these low-cost instruments can also detect them.

A key challenge in breath-based disease detection, however, is the widespread use of antibiotics in livestock management. Antibiotics remain a cornerstone of BRD treatment, often administered at first suspicion of illness and, in some cases, prophylactically in high-risk groups such as recently weaned calves [29]. While effective in controlling bacterial infections, their potential influence on breath biomarkers remains an open question. If VOC shifts caused by antibiotics obscure or mimic disease-related signals, it may complicate diagnostic accuracy.

Recent studies in human breathomics have demonstrated the presence of antibiotic metabolites in exhaled breath, suggesting that pharmaceutical intervention can directly alter VOC profiles [30]. This raises concerns about whether breath-based diagnostics truly capture pathology or if treatment effects inadvertently shape biomarker interpretation. Understanding how drugs, or indeed vaccination, modify breath composition is essential for ensuring reliable disease detection.

In this study, we investigate breath-based detection of BRD within a farm setting where disease management involved antibiotic treatment. Using online mass

spectrometry, we analysed breath samples from 65 calves to characterise VOC patterns in diseased and healthy animals, assessing the potential for breath-based disease detection, including piloting the use of low-cost sensors to determine whether they are sufficiently sensitive to any of the identified markers of disease (phase 1). To further probe the influence of antibiotics, we conducted a secondary trial (phase 2) administering treatment to healthy calves, tracking breath composition over multiple time points.

2. Methods

2.1. Online breath sampling

Breath samples were collected using a custom-built polycarbonate mask which was 15 cm in diameter and 15 cm long. The open end of the cylinder was covered with a silicone lid (Dunelm) with an aperture of 8 cm, to form an effective seal around the animal's muzzle. At the end of the cylinder, a charcoal respirator filter (3M Gas & Vapour filter, GF22 A2, Arco Limited, Hull, UK) was fitted to help limit the concentration of VOCs in the air entering the mask. Exhaled breath was sampled through a ¼" OD tube (I.D. 1/8") which connected to the base of the mask and passed through a Teflon filter to remove any particulates from the sampled air. Flexible PFA tubing was used for the first metre of sample and then the air going for online analysis was carried along a 6 m, ¼" OD Sulfinert® coated stainless steel tube (I.D. 1/8"). The tubing was inserted into a custom-built heating sleeve (Signal Group Ltd, Camberley, UK) set to 140 °C. This maintained an internal air temperature of 45 °C, which prevented condensation and limited VOC adsorption onto the tube walls. The flow rate was maintained at 7 L min⁻¹ under a pressure of 800 mbar, both of which were measured, together with air temperature via a thermal mass flowmeter (TSI Model 4040, USA), mounted downstream of the gas analysers. The full sampling setup is shown in Fig 1.

Air from the sample line was sub-sampled by a proton transfer reaction time of flight mass spectrometer with quadrupole ion guide (PTR-QiTOF, IONICON Analytik GmbH, Austria) [31]. The instrument was operated with a drift tube pressure, voltage and temperature of 3.7 mbar, 830 V and 80 °C, respectively. These settings ensured the ratio between electric field (E) and number density of gas molecules within the drift tube (N) was maintained at a value of 120 Td. H₃O⁺ reagent ions were used to detect VOCs with a proton affinity greater than that of water.

The PTR-Qi-TOF was calibrated at both the beginning and end of each measurement period using a multicomponent gas standard (Apel-Riemer Environmental Ltd). Following standard practice [32,33], an instrument-specific transmission curve was derived from the known concentrations of the calibrated compounds. This curve was then combined with published reaction rate constants to convert ion signal intensities to concentrations expressed in milligrams per metre cubed (mg m⁻³) for all detected ions. The transmission-based quantification method carries an associated uncertainty of approximately 25% [32].

Measurements of carbon dioxide (CO₂), were made using a MIRO MGA10-GP gas analyser (MIRO Analytical, Wallisellen, Switzerland). This instrument, which uses direct laser absorption spectroscopy, subsampled downstream of the PTR-QiTOF. The MIRO sampled at a rate of 1 Hz, with data logged directly to the PTR-QiTOF. CO₂ is also detectable by PTR-QiTOF instruments at high concentrations due to endothermic proton transfer reactions occurring at the transition point between drift tube and time-of-flight chamber. This is enhanced in instruments with a quadrupole ion guide due to the higher energies present in this region [25]. The CO₂ signal is typically suppressed by tuning the source valve, but here a higher CO₂ signal was desirable to allow synchronisation between the two instruments by searching for the maximum in a cross-covariance of the two CO₂ signals, with the difference typically 3 seconds. The higher resolution (2 Hz) measurements of CO₂ made by the PTR-QiTOF were used for the analysis following calibration against the MIRO data. Allowing a higher CO₂ signal came at the cost of compromising the acetaldehyde signal at (C₂H₄O)H⁺, which sits on the shoulder of the much larger CO₂ peak.

2.2. Emission rates of breath volatiles

The emission rate of volatiles exhaled on the breath of calves (E_{exhaled}) was calculated in units of mass per animal per hour (e.g., mg animal hr⁻¹), depending on compound abundance, as [34]:

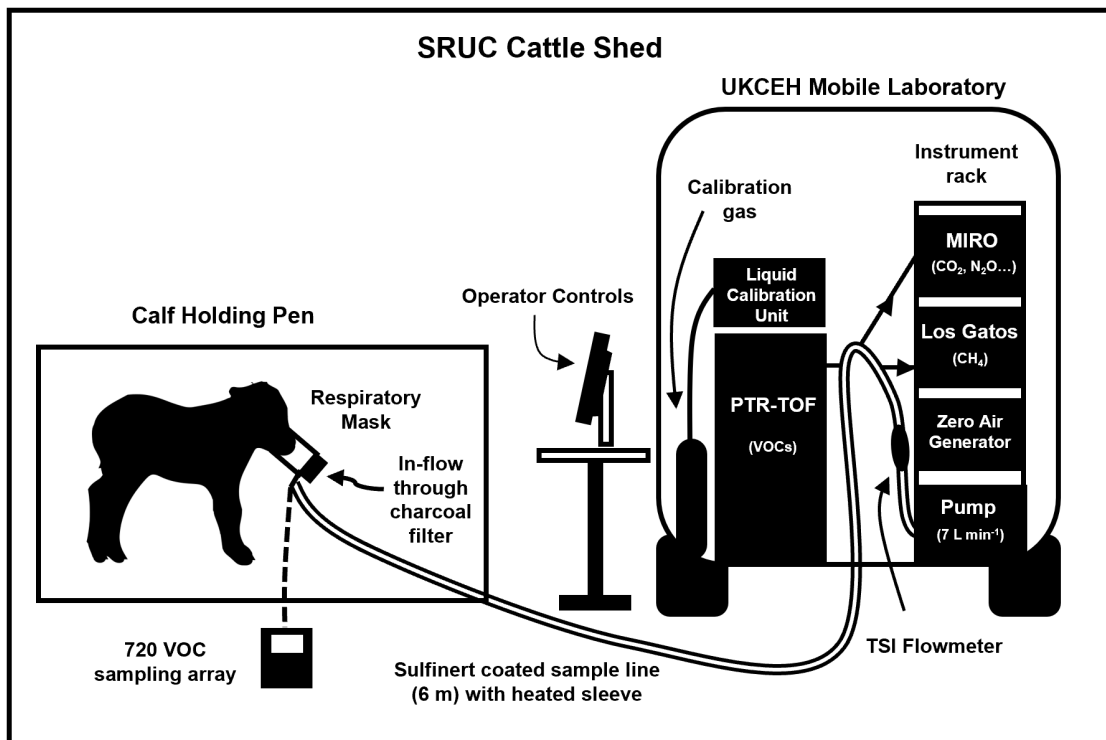


Fig 1. Experimental setup comprising a mobile laboratory housing the gas analysers and a 6 m heated sample line connected to a custom-made breath-sampling mask. Data acquisition was operated by trained farm technicians, who initiated sampling from the side of the cattle pen.

<https://doi.org/10.1371/journal.pone.0351838.g001>

$$E_{\text{exhaled}} = (x_{\text{breath}} - x_{\text{bg}}) \cdot TV \cdot RR$$

Where x_{breath} is the concentration of the target VOC (e.g., mg m^{-3}) measured from the mask and x_{bg} is the concentration of target VOC measured from a closed mask immediately prior to fitting to the animal, which forces air through the charcoal filter and acts as a blank. Mask and mask background were both measured for a period of 3 minutes for each animal sample, with the median value used in the calculation. The tidal volume (TV) was calculated for each animal and based on the value of $8 \times 10^{-6} \text{ m}^3$ per kg of body weight from Dißmann et al. [35]. Cattle were weighed at the start and end of the study, and interim values estimated based on a linear interpolation between the two weights. Respiration rates were calculated for each animal by counting the average breaths per minute for each sample which were clearly visible in the CO_2 data (see Fig 2B).

2.3. Low-cost sensors – VOC sensing array

As part of a proof-of-concept trial, a Model 720 VOC Analyser (RoboScientific Ltd, UK) was used to assess the feasibility of breath sampling in calves. The analyser was connected to the outflow tubing of the breath sampling mask and was trialled on several animals during the study period, rather than being applied to the full experimental cohort. Sampling was conducted in two stages: first, four replicate background air samples were collected over a two-minute period with the mask in blanked configuration. This was followed by breath sampling immediately after fitting the mask to the calf, again comprising four replicates over a two-minute period.

The 720 VOC Analyser comprises an array of 24 individual sensors, each embedded with distinct organic semiconducting materials. During each sampling event, the analyser captures sensor responses characterised by parameters

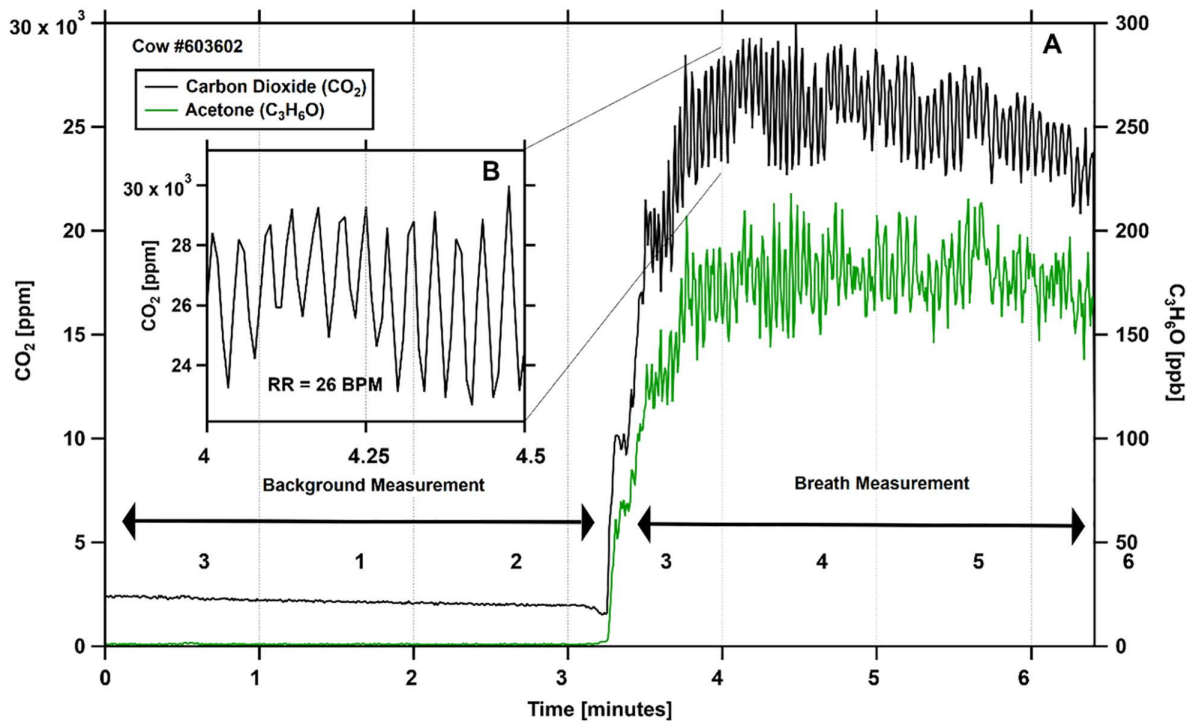


Fig 2. Example breath measurement, showing the background phase (0–3 minutes) and the breath phase (3–6 minutes). Panel B provides a close-up of the CO₂ signal used to calculate the respiration rate for each animal.

<https://doi.org/10.1371/journal.pone.0351838.g002>

such as peak height, integrated area under the response curve, absorption and desorption rate, as selected by the operator. These multivariate data were analysed both individually, for example, to compare specific sensor responses with known VOCs identified via PTR-QiTOF, and collectively, to assess changes in breath profiles over time. Cosine similarity, expressed in degrees, was used to quantify the divergence between each diseased day and the healthy baseline measurement (see section below for definitions), providing a measure of how VOC signatures evolved throughout the course of disease. Cosine similarity is defined as:

$$\theta = \cos^{-1} \left(\frac{\mathbf{A} \cdot \mathbf{B}}{|\mathbf{A}| |\mathbf{B}|} \right) \times \left(\frac{180}{\pi} \right) \quad (2)$$

where **A** and **B** denote the feature vectors extracted from the VOC profiles of two individual breath samples. The resulting angle θ represents the degree of similarity between the vectors: 0° indicates a perfect match, while 180° indicates complete opposition.

2.4. Animals, health assessment and treatments

The study was conducted under ethical approval from SRUC's Animal Experiments Committee (Approval number: AEX 2024-024 DAI).

A total of 65 calves completed the trial, aged between 12 and 86 days, comprising 30 heifers and 35 steers. Each animal was born to a Holstein dam—a dairy breed—but sired by bulls representing three beef breeds: Hereford, Aberdeen Angus, and British Blue [36]. In compliance with the UK Home Office Project Licence, animals were checked by a veterinarian and returned to the farm stock. No animals were euthanised or sacrificed specifically for the purposes of this study.

During the trial animals were fed 4 litres of milk replacer (Carr's Billington Vitality calf milk) twice daily at 08:00 and 15:00 and were given ad libitum access to barley straw and starter pellets (Davidson's rapid starter pellets, 2359). Health status was assessed each morning using the modified Wisconsin scoring system [37], which grades five clinical indicators—rectal temperature, nasal discharge, eye discharge, ear droop, and cough—on a scale of 0–3. For the purposes of this study, a calf was classified as diseased only when both the cumulative score reached five or more and rectal temperature exceeded 39.5 °C. This combined threshold was used to reduce misclassification arising from transient environmental irritants or mild non-respiratory conditions that can elevate individual components of the clinical score. Because the calves were group-housed, faecal consistency was not included, as faeces could not reliably be attributed to specific individuals. Animals identified as either healthy controls or meeting the criteria for respiratory disease during the morning assessment were sampled later the same day, following the breath-sampling protocol outlined below. Breath sampling was non-invasive and did not require anaesthesia or sedation. Health monitoring was carried out under Home Office Licence, with appropriate end points set for each procedure allowing animals to be withdrawn from the trial in the case they suffered any ill-effects of the procedure. However, in this trial, no end points were ever reached. Animals were handled by trained farm personnel, and procedures were designed to minimise stress and disturbance.

The number of breath samples that could be collected from each animal was determined by the conditions of the Home Office licence governing the study. Each calf could contribute up to five healthy breath samples throughout the trial period. If an animal met the disease criteria, up to five further breath samples could be taken on consecutive days following disease onset, with a maximum of two such disease episodes sampled per calf. These regulatory constraints dictated the feasible sampling frequency for each individual and explain why the number of available breath measurements varied across animals.

Immediately after breath sampling, calves diagnosed with respiratory disease were treated according to standard farm practice and all treatment histories are reported in the associated data publication. Treatment typically consisted of an intramuscular injection of meloxicam (Metacam®, Boehringer Ingelheim) alongside oxytetracycline dihydrate (Alamycin® LA 300, Norbrook Laboratories), administered into the gluteal muscles of the hindquarters. In a small number of cases where clinical signs did not improve sufficiently, further treatment with gamithromycin (Zactran®, Boehringer Ingelheim) or amoxicillin trihydrate–clavulanic acid (Synulox®, Zoetis) was provided. Calves were not vaccinated prior to the study, and polymerase chain reaction (PCR) testing was not performed, meaning that the specific pathogens responsible for each disease event could not be identified. Consequently, some respiratory episodes may have involved viral, bacterial, or mixed infections, or systemic conditions that mimicked BRD. This reflects the reality of on-farm diagnosis and mirrors the context in which breath-based disease detection technologies would ultimately be deployed.

2.5. Assessment of antibiotic breath metabolites

To evaluate the impact of therapeutic antibiotic treatment on breath VOC profiles, a second trial was conducted. A cohort of 10 healthy Aberdeen Angus Cross calves (seven males, three females, aged 28–43 days), all from a dairy dam, was selected. Daily breath samples were collected over two consecutive days to establish a baseline. On the third day, animals received a long-acting, broad-spectrum injectable antibiotic containing 300 mg/mL of oxytetracycline dihydrate as the active ingredient (Alamcin® LA 300). This was the same drug used during the initial on-farm trials, providing a consistent pharmacological reference across study phases. The formulation also includes excipients such as magnesium oxide and sodium formaldehyde sulfoxylate, which contribute to its extended-release profile. A dosage of 1 mL per kg of body weight was administered intramuscularly into the hindquarters. Following treatment, breath samples were collected at approximately 1, 24, 48, 72, and 96-hours post-administration to monitor VOC changes over time. The same modified Wisconsin health scoring system was adopted (daily scoring) to confirm that calves remained healthy throughout this trial period.

3. Results and discussion

3.1. Breath sampling

During the main study, measurements were made from 65 cattle, from two batches, between May-July and Sep-Oct 2024. A total of 398 breath samples were taken using the mask setup described in Section 2.1.

[Fig 2a](#) shows a typical breath sample of CO₂ and acetone/propanal ((C₃H₆O)H⁺). The first three minutes represent the background period where the mask was sealed with a silicone lid to force air through the charcoal filter and provide a sample blank. The next three minutes show the period where the mask was placed on the calf to obtain the breath sample. The arrows indicate the portion of the data that were averaged (median) to provide values of x_{breath} and x_{bg} . The CO₂ signal shown was measured by the PTR-QiTOF and calibrated against the CO₂ signal obtained from the MIRO.

In total, 21 disease events were captured from 20 individuals, with 103 breath samples captured during the 5-day diseased period. Healthy breath samples were carefully screened to remove any samples where the animal went on to become diseased in the subsequent 4 days. This left 204 ‘true’ healthy samples, taken from 41 individuals.

The PTR-TOF detected 86 ions that were consistently present in the breath of cattle. Molecular formula could be assigned to 55 of these ions with the remaining 31 reported as their protonated mass-to-charge ratio and classed as ‘unidentified’. The full list of compounds and molecular formula are listed in Table S2 in [S1 File](#) of the Supplementary Information.

3.2. Disentangling growth effects from potential disease signals in calf breath VOCs

During the early weeks and months of a calf’s life, rapid growth significantly influences the emission of volatile organic compounds (VOCs) in the breath, largely due to developmental changes such as increased lung capacity. These growth-related changes can be substantial [36] and must be accounted for to accurately distinguish disease-induced alterations in the volatilome from those caused by natural growth.

[Fig 3A](#) presents the growth curve of CO₂ emission rates in the breath of healthy calves. Green data points represent measurements from ‘true’ healthy animals, those with no disease within ±4 days of sampling. The fitted curve, along with the 95% confidence interval ($1.96 \times \sigma$), shows that CO₂ emission rates nearly double over the monitored age range, emphasising the necessity of age correction when evaluating breath-based disease biomarkers. When breath data obtained from calves during episodes of disease (e.g., 5 consecutive days post-onset, shown in red) are added, only one sample falls outside the healthy confidence interval. This suggests that CO₂ emissions are not significantly affected by respiratory disease in this cohort.

[Fig 3B](#) illustrates the same analysis for the (CH₂O)H⁺ ion, attributed to formaldehyde, one of the most abundant compounds emitted from both healthy and diseased animals. Among the diseased samples, 32 exceed the confidence interval, corresponding to 15 individuals, from a possible 21. Additionally, 19 healthy samples from nine individuals also fall above the threshold.

In [Fig 3C](#), the (C₃H₆O)⁺ ion is shown, which likely reflects acetone/propanal detected directly at its monoisotopic mass (m/z 58.0419) via charge transfer from residual O₂⁺ ions present as impurity species in the H₃O⁺ drift tube. A total of 31 diseased samples (16 individuals) exceeded the threshold, compared to 18 healthy samples (10 individuals).

The (C₅H₁₀O)H⁺ ion in [Fig 3D](#) relates to a possible mix of 3-methylbutanal, 2-pentanone, and pentanal. This ion showed 27 threshold exceedances over the five-day diseased period relating to 15 diseased animals and 13 exceedances relating to 13 healthy animals.

[Table 1](#) summarises the performance of the top 15 ions detected by PTR-QiTOF, ranked by the number of diseased individuals exhibiting threshold crossings. For example, C₂H₄O⁺, likely acetaldehyde formed via direct charge transfer from O₂⁺, was detected in 13 diseased individuals. This ion proved to be a more reliable marker for acetaldehyde than the protonated form (C₂H₄O)H⁺, which, as discussed in Section 2.1, was confounded by the dominant (CO₂)H⁺ peak. In

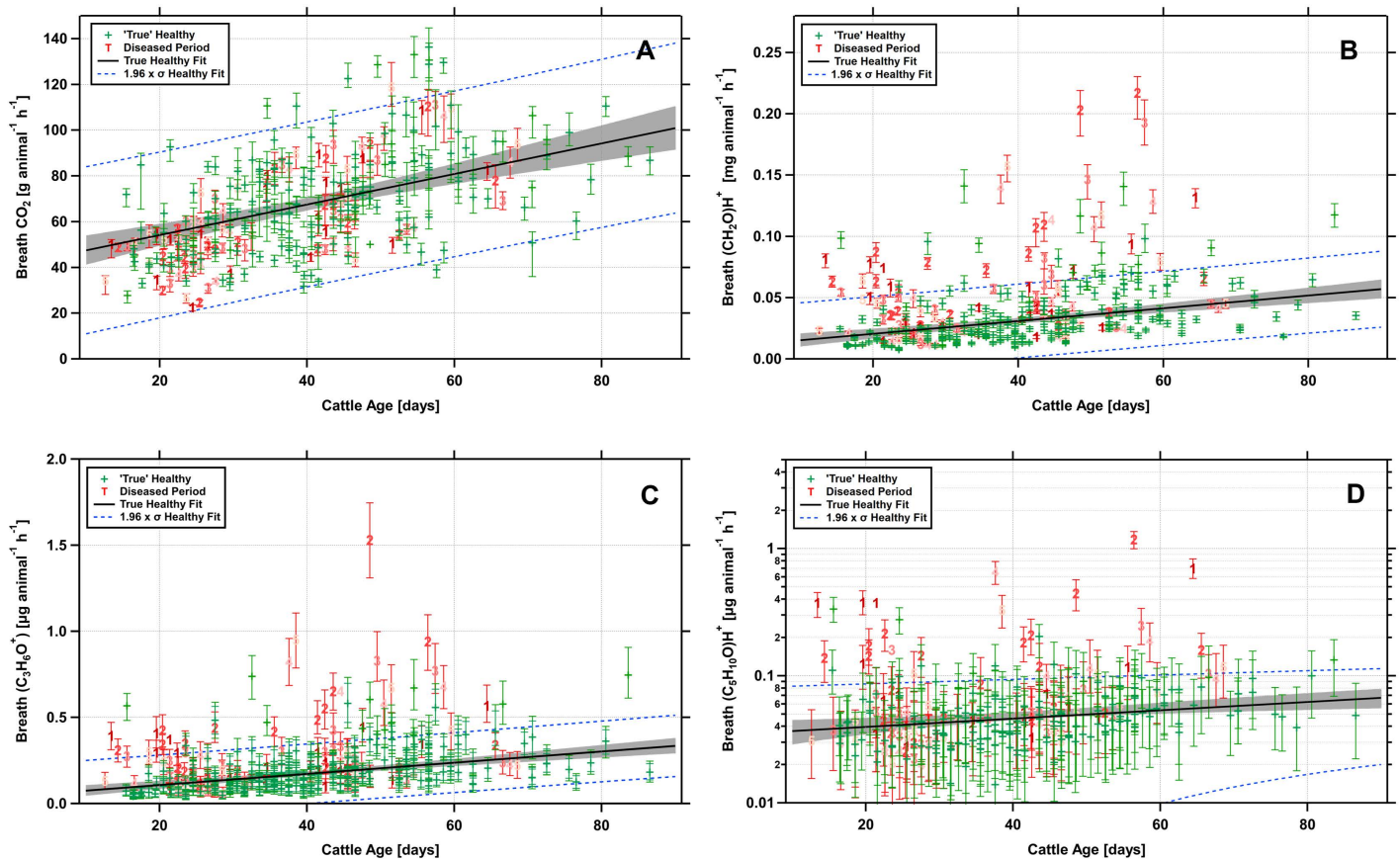


Fig 3. Breath emission rates of CO_2 (panel A), formaldehyde $(\text{CH}_2\text{O})\text{H}^+$ (panel B), acetone/propanal $(\text{C}_3\text{H}_6\text{O})^+$ (panel C), and $(\text{C}_5\text{H}_{10}\text{O})\text{H}^+$ (panel D) plotted against calf age. Green data points represent measurements from “true” healthy calves (i.e., no recorded disease within four days before or after sampling). Red data points represent breath samples collected during a five-day window following a respiratory disease event. Red symbols are labelled to indicate the specific day post-onset (days 1–5) on which the sample was taken. Error bars indicate the interquartile range.

<https://doi.org/10.1371/journal.pone.0351838.g003>

addition, several fragment ions, including $(\text{C}_3\text{H}_2)\text{H}^+$, $(\text{C}_3\text{H}_4)\text{H}^+$, and $(\text{C}_4\text{H}_6)\text{H}^+$, showed consistent levels across samples, suggesting potential as supporting markers, although their parent compounds could not be definitively identified.

3.3. Age-Normalised emission profiles across disease days (D1 to D5)

All measured emission rates were normalised using their respective growth response curves. The coefficients and confidence intervals associated with these curves are provided for each of the 86 identified ions in Table S1 in [S1 File](#) of the Supplementary Information.

To investigate how breath volatiles change over the course of the five days following disease onset, the normalised data were aggregated (using the median) for both the healthy control group and each day of the diseased period. These results are presented in [Fig 4](#) for Formaldehyde (Panel A), Acetone/Propanal (Panel B), and $(\text{C}_5\text{H}_{10}\text{O})\text{H}^+$ ion (Panel C). A Mann-Whitney U test was applied to assess statistical differences between each diseased day and the healthy control population.

All three markers exhibited broadly similar temporal profiles, beginning with statistically significant elevations in formaldehyde and acetone/propanal on Day 1 ($p < 0.01$), while no significant difference was observed for $\text{C}_5\text{H}_{10}\text{O}^+$ at this

Table 1. Summary of the top 15 PTR-QiTOF ions elevated above the healthy 95% confidence interval, listed by decreasing prevalence across diseased individuals. For each ion, we report the monoisotopic m/z, the molecular formula (when a unique formula could be assigned), a putative identification (where possible), the total number of diseased samples in which an exceedance occurred, the number of diseased individuals contributing those exceedances, and the counts by disease day (D1–D5) post-diagnosis. Ions labelled “unknown” are peaks for which no unambiguous formula match could be made (e.g., fragment ions or compositions outside the element set used for matching), which is typical for high-resolution PTR-TOF datasets.

m/z	Formula	Possible ID	#Diseased Samples	#Diseased Individuals	# on D1	# on D2	# on D3	# on D4	# on D5
58.041	C ₃ H ₆ O ⁺	Acetone/propanal (via O ₂ ⁺ charge transfer)	31	16	7	11	5	4	4
31.018	(CH ₂ O)H ⁺	Formaldehyde	32	15	8	11	5	4	4
87.08	(C ₅ H ₁₀ O)H ⁺	3-methylbutanal, 2-pentanone, Pentanal	27	15	6	11	2	4	4
44.024	C ₂ H ₄ O ⁺	Acetaldehyde (via O ₂ ⁺ charge transfer)	32	14	7	10	7	4	4
56.04427	56.0443	unknown	24	14	6	8	4	4	2
61.05348	61.0535	unknown	26	14	6	11	2	4	3
39.023	(C ₃ H ₂)H ⁺	Fragment	26	13	6	10	3	4	3
40.02629	40.0261	unknown	27	13	6	10	4	4	3
41.03858	(C ₃ H ₄)H ⁺	Fragment	27	13	6	10	3	4	4
53.00223	53.0022	unknown	29	13	7	10	6	3	3
55.054	(C ₄ H ₆)H ⁺	Fragment	23	13	5	7	3	4	4
56.057	56.057	unknown	23	13	5	7	3	4	4
59.049	(C ₃ H ₆ O)H ⁺	Acetone/propanal	26	13	6	10	3	4	3
60.05248	60.0524	unknown	26	13	6	10	3	4	3
48.00337	(CH ₄ S)H ⁺	Methanethiol	23	12	5	8	4	4	2

<https://doi.org/10.1371/journal.pone.0351838.t001>

stage. On Day 2, all compounds showed their largest deviations from healthy controls, with highly significant increases for all three markers ($p < 0.001$). This elevated response persisted into Day 3, where formaldehyde and acetone/propanal remained strongly significant ($p < 0.001$) and (C₅H₁₀O)H⁺ retained a more modest but still significant difference ($p < 0.05$). By Day 4, formaldehyde and acetone/propanal remained elevated ($p < 0.04$), whereas (C₅H₁₀O)H⁺ had returned to baseline levels and was no longer significantly different. The supplementary Information contains similar visualisations for the remaining compounds listed in Table 1 (figures S1-S3 in S1 File).

The temporal profile of VOC emission rates across the 5-day diseased period mirrors the distribution of threshold exceedances observed for the three key compounds. As illustrated in Fig 3, each breath sample is annotated by disease day (1–5), revealing consistent day-wise variation in marker elevation. Among the top three markers, 22% of all threshold exceedances occurred on Day 1, rising sharply to 42% on Day 2, the peak response, before declining to 11%, 15%, and 10% on Days 3, 4, and 5, respectively. These data suggest that the most pronounced perturbations in breath VOCs occur within the first 48 hours following onset of clinical symptoms, with Day 2 consistently representing the strongest signal across individuals.

3.3.1. Non threshold exceedances. Of the 21 diseased animals, breath marker exceedances were detected in up to 16 individuals. Importantly, these 16 cases represent the complete subset of diseased animals that were detectable using any combination of these or other markers. In other words, there was no additional discriminatory signal in the remaining five BRD-positive individuals that could be recovered through either linear or non-linear combinations of the available markers, when comparing against the healthy population detection thresholds.

Among the five that exhibited no threshold exceedances, further inspection revealed that one animal (#209498) lacked a measurement on Day 2, the time point associated with the highest probability of exceedance events, and thus a key opportunity for detection was missed.

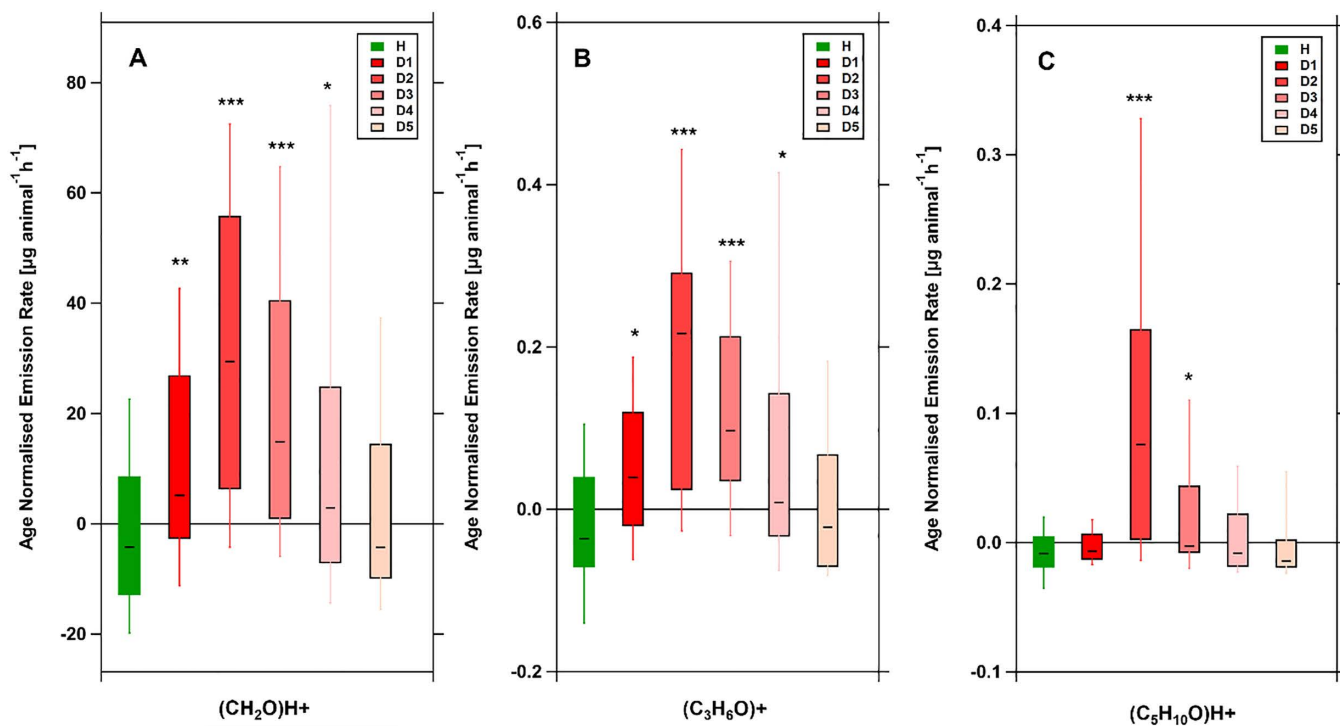


Fig 4. Box-and-whisker plots of age-normalised breath emission rates of formaldehyde (A), acetone/propanal (B), and (C₅H₁₀O)H⁺ (C) during healthy and diseased periods (progressing from D1 to D5). Asterisks indicate statistical significance: **p* < 0.001, ***p* < 0.01, **p* < 0.05.**

<https://doi.org/10.1371/journal.pone.0351838.g004>

Fig 5 shows the time series data for animal #613315. Grey bars indicate the relative health score, with Day 1 marking the onset of the diseased period. While all three markers peaked on Day 2 and returned to baseline by Day 3, their absolute emission levels remained below the population-derived threshold (solid line), resulting in no exceedance events for this animal. This highlights a key limitation of population-based thresholds and suggests that more sensitive or individualised monitoring strategies may yield higher diagnostic resolution.

In contrast, animal #504941 exhibited no elevation in any of the three key ions during the diseased period and received only a single 1.5 mL dose of Metacam, with no antimicrobial treatment administered. Similarly, animals #109490 and #713323, although clinically diagnosed with respiratory disease, did not meet the criteria for antibiotic treatment. Both animals showed no elevation in (C₅H₁₀O)H⁺ levels. Modest increases in formaldehyde and acetone/propanal were observed on both Days 1 and 2 for #109490, and on Day 2 for #713323 (see Fig. S4 in S1 File), but in all cases, these remained well below the population threshold. The absence of antimicrobial intervention in these animals suggests that the observed VOC changes reflect a physiological response to disease rather than a pharmacological effect. In contrast, for those animals that did receive antibiotics, the most pronounced increases in VOC emissions were consistently seen on the second day of the diseased period, after treatment had been administered on Day 1. This timing raises the possibility that antimicrobial administration may act as a confounding factor in VOC-based disease profiling.

3.4. Antibiotic trial

To evaluate the potential confounding influence of antimicrobial treatment, we conducted a second trial in which a cohort of 10 healthy animals received antibiotics. At the onset of the trial, three of the 10 calves scored diseased within the first two days and were therefore excluded from the study. Fig 6 presents a principal component analysis (PCA) of breath

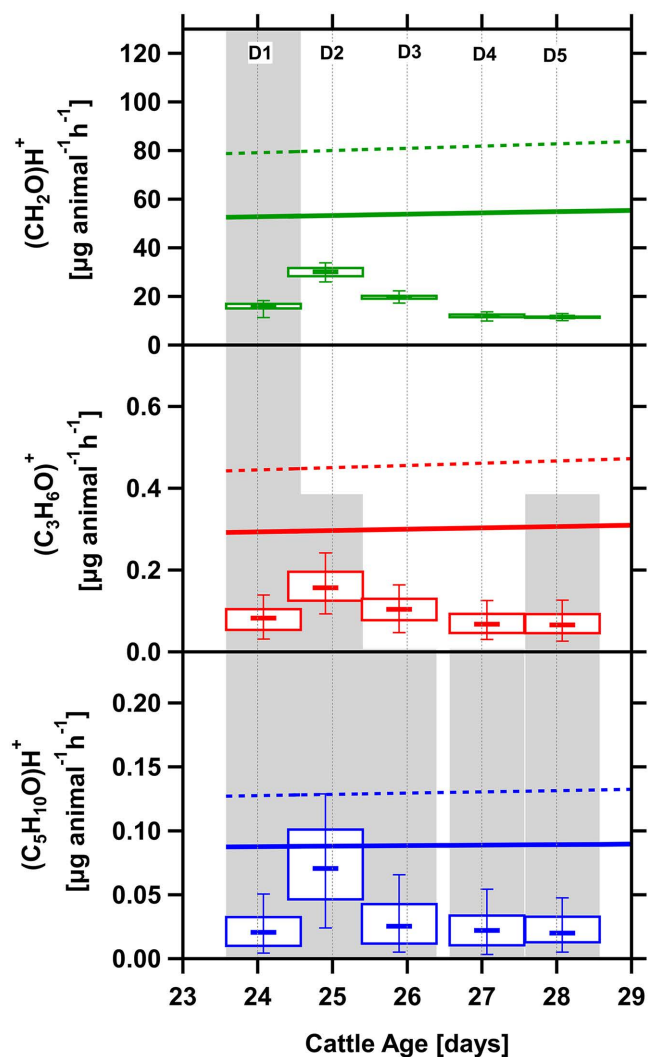


Fig 5. Box-and-whisker plots (10th, 25th, 50th, 75th, and 90th percentiles) of breath emission rates for formaldehyde, acetone/propanal, and the $(C_5H_{10}O)H^+$ ion in calf #613315 across different ages. Grey bars represent the relative health score. D1–D5 denote the five days following disease onset. Solid lines indicate the linear fit of the average breath emission rates for the ‘true’ healthy cohort, while dashed lines represent the 95% confidence intervals.

<https://doi.org/10.1371/journal.pone.0351838.g005>

samples collected from the remaining seven (4 male, 3 female) healthy cattle before and after antimicrobial treatment. Samples obtained on Days 1 and 2 ($n=14$), prior to antibiotic administration, cluster together in the lower left quadrant, representing the pre-treatment volatilome profile. Within just one hour of administering the antibiotic, the samples diverge markedly from this baseline, indicating a pronounced shift in breath chemistry. Notably, a gradual return toward the pre-treatment cluster begins around 72 hours post-injection and continues through to 96 hours, suggesting a transient but substantial alteration in the volatilome following treatment.

To further quantify these effects, the three most discriminatory ions identified in the initial trial were re-evaluated in this cohort. After age normalisation, emission rates were averaged for each time point to facilitate statistical comparisons between the pre- and post-treatment periods. [Fig 7](#) displays the resulting median normalised emission rates across the group, while individual animal trajectories are provided in the Supplementary Information (Figs S5–S31) in [S1 File](#).

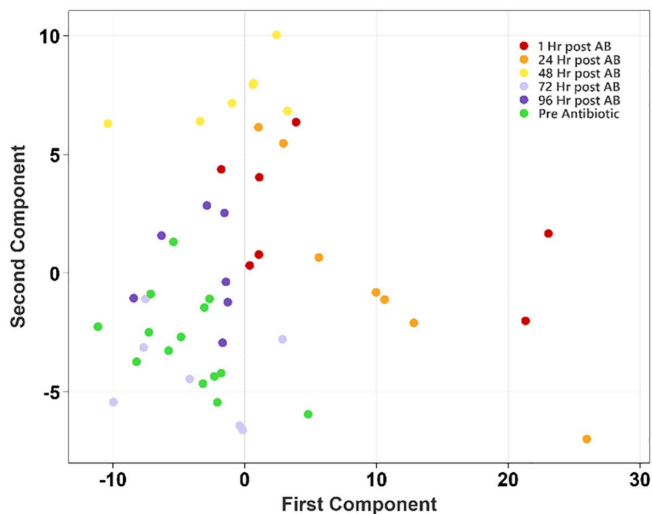


Fig 6. Principal Component Analysis (PCA) of breath samples from seven healthy calves collected prior to treatment (green) and at 1, 24-, 48-, 72-, and 96-hours post-treatment with oxytetracycline dihydrate (LA300® Alamyacin) antibiotic. Pre-treatment samples were collected across two days, resulting in 14 data points for that group, whereas all post-treatment time points contain seven samples each, representing single sampling events.

<https://doi.org/10.1371/journal.pone.0351838.g006>

Following administration of oxytetracycline dihydrate (Alamyacin® LA 300), a transient increase in sulphur-containing VOCs was observed in the exhaled breath of treated cattle. Notably, dimethyl sulfide (DMS), Fig 7, panel D, exhibited statistically significant elevations at 1 hour ($p=0.0159$) and 24 hours ($p=0.0250$) post-injection, relative to baseline levels established over the two days prior to treatment. These findings were derived using the Mann-Whitney U test across a cohort of seven animals, with emission rates normalised against healthy cohort growth response curves from the initial phase 1 study.

While the active ingredient of the antibiotic, oxytetracycline dihydrate, is not sulphur-based, the formulation does include sodium formaldehyde sulfoxylate, a sulphur-containing excipient. Therefore, it is plausible that the observed DMS arises from rapid metabolic processing of this compound.

Other VOCs, including $(C_5H_{10}O)H^+$ (Fig 7, Panel C), also showed significant changes at 1 hour ($p=0.0005$) and marginal significance at 24 hours ($p=0.0309$), but not thereafter. In contrast, compounds such as formaldehyde (Panel A) and acetone/propanal (Panel B) reached significance only at 24 hours, with p -values rising above the 0.05 threshold at later time points.

Crucially, none of the monitored compounds remained significantly elevated beyond 24 hours. This is in marked contrast to findings from the phase 1 study, in which animals were treated while actively diseased. In that context, VOCs such as formaldehyde and acetone/propanal remained significantly elevated for up to 72 hours post-treatment. The absence of sustained VOC elevation in the current study likely reflects the fact that animals were clinically healthy at the time of antibiotic administration. This distinction underscores the influence of underlying disease processes on the breath volatome and highlights the importance of physiological context when interpreting VOC-based diagnostics.

3.5. Receiver operating characteristic analysis of key marker ions

To evaluate the diagnostic accuracy of the most promising breath biomarkers, Receiver Operating Characteristic (ROC) curves were generated for three ions exhibiting the highest classification potential: $(CH_2O)H^+$ (formaldehyde), $(C_3H_6O)^+$ (acetone/propanal), and $(C_5H_{10}O)H^+$.

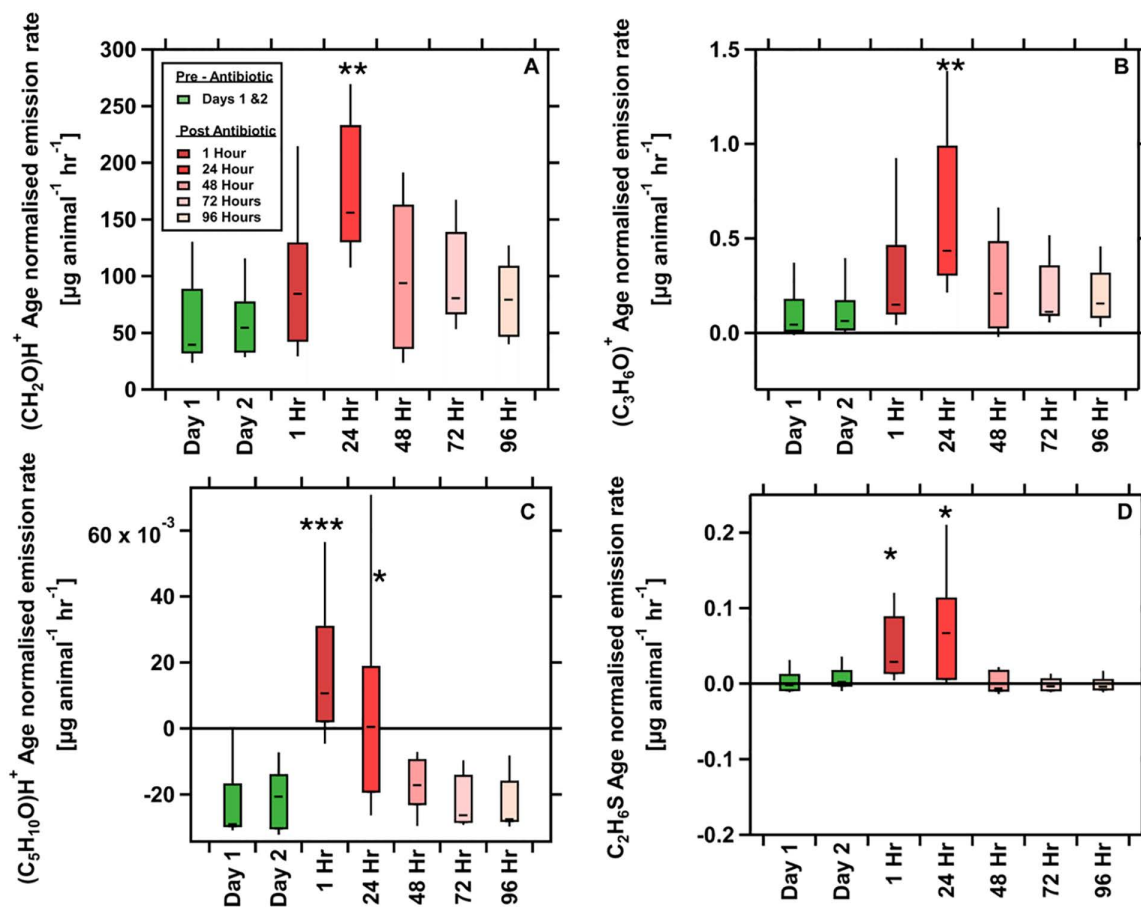


Fig 7. Box and whisker plots showing the emission rates of formaldehyde (A), acetone/propanal (B), $\text{C}_5\text{H}_{10}\text{O}$ ion (C) and dimethyl sulphide (D) measured from the breath of seven healthy cattle before (Days 1 and 2) and after (1, 24, 48, 72, 96 hours) injection with oxytetracycline dihydrate (Alamycin® LA 300). Emission rates are age normalised by subtracting the growth response curves discussed in Section 3.2. Asterisks indicate statistical significance: * $p < 0.001$, ** $p < 0.01$, * $p < 0.05$.**

<https://doi.org/10.1371/journal.pone.0351838.g007>

ROC curves plot the true positive rate (sensitivity) against the false positive rate ($1 - \text{specificity}$) across a range of detection thresholds, offering a comprehensive view of each biomarker’s discriminative ability. Classification performance is quantified using the Area Under the Curve (AUC), where a value of 1.0 indicates perfect discrimination and 0.5 denotes no better than random chance.

To assess variability, bootstrap resampling ($n = 1000$ iterations) was performed to compute 95% confidence intervals for each ROC curve. These intervals were derived from the 2.5th and 97.5th percentiles of the resampled ROC distributions.

Based on data from the antibiotic trial, the ROC analyses shown in Fig 8 were conducted separately for breath samples collected on Day 1 (pre-treatment, panels A-C) and Day 2 (post-treatment, Panels D-F) to assess performance changes following antimicrobial exposure.

On Day 1, pre-treatment data showed moderate discriminative power for formaldehyde (CH_2O , m/z 31.018, Panel A) with an AUC of 0.66 (95% CI: 0.53–0.77), and a similar result for acetone/propanal ($\text{C}_3\text{H}_6\text{O}^+$, m/z 58.041, Panel B) with an AUC of 0.65 (0.52–0.77). In contrast, the ($\text{C}_5\text{H}_{10}\text{O}$) $^+$ ion (m/z 87.08, Panel C) yielded an AUC of 0.45, indicating no discriminatory ability. This aligns with the absence of statistically significant differences in age-normalised emission rates between healthy calves and those with early-stage disease, confirming that ($\text{C}_5\text{H}_{10}\text{O}$) $^+$ is not a biomarker for BRD. It is

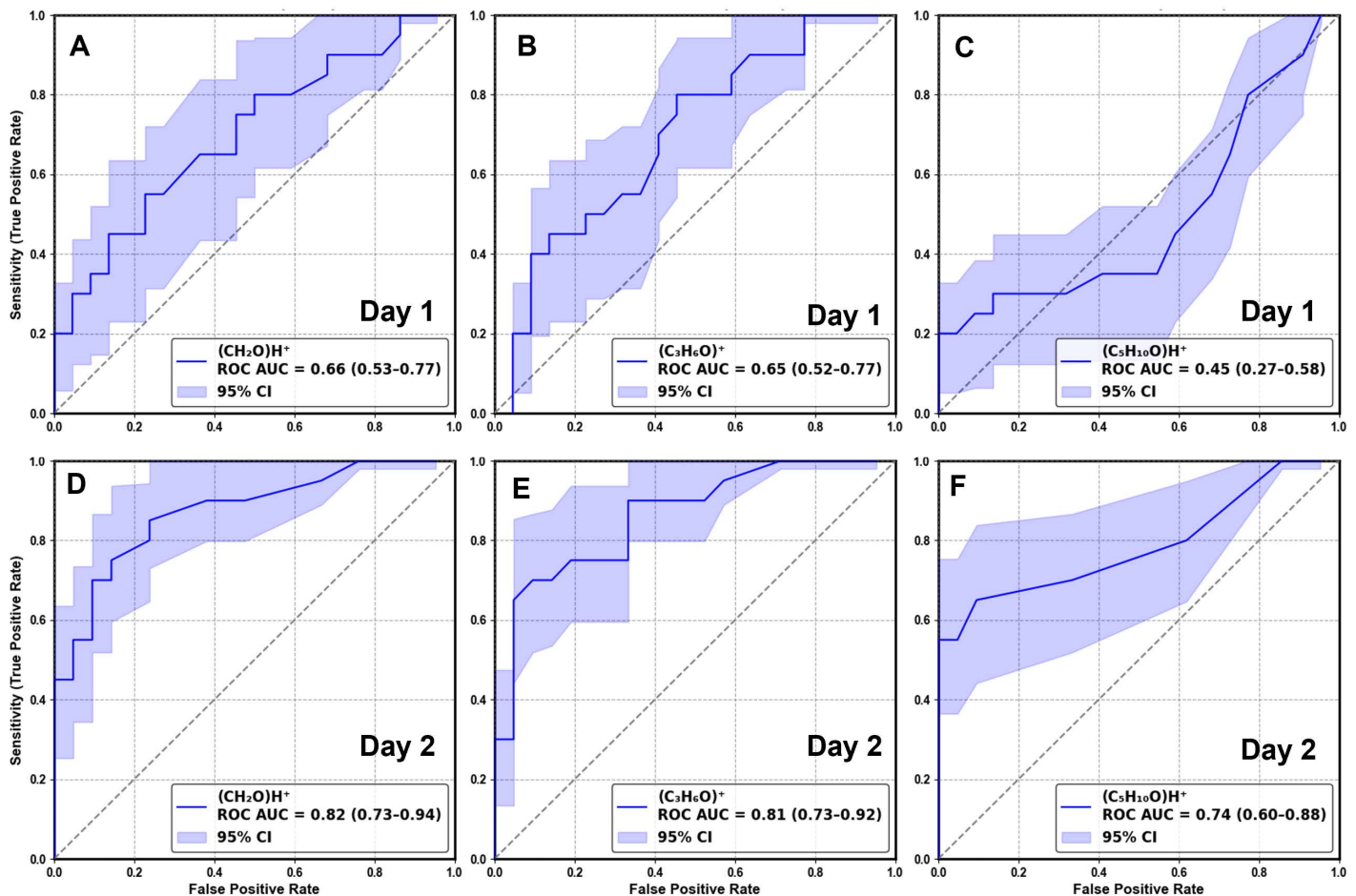


Fig 8. Receiver Operating Characteristic (ROC) curves for the three best-performing ions: formaldehyde ((CH₂O)H⁺), acetone/propanal ((C₃H₆O)H⁺), and a likely mixture of pentanal, 2-pentanone, and 3-methylbutanal ((C₅H₁₀O)H⁺). The blue lines represent mean ROC curves across bootstrap iterations, while the shaded bands indicate 95% confidence intervals (CI) derived from 1000 bootstrap resamples. The area under the curve (AUC) is reported for each ion, providing a quantitative measure of its classification performance. Panels A-C show ROC curves for Day 1, pre-treatment and Panels D-F show ROC curves for Day 2, post treatment.

<https://doi.org/10.1371/journal.pone.0351838.g008>

important to note, however, that animals were sampled at the very first clinical signs of disease, as determined through daily health scoring. This early intervention likely limited the severity and metabolic expression of BRD at the time of sampling. Had the disease been allowed to progress untreated to Day 2, the biomarker signal, particularly for BRD-associated volatiles, may have been further amplified, potentially resulting in higher classification performance. For example, animals #109490 and #713323 both showed larger formaldehyde and acetone/propanal emission values on day 2 of the diseased period, compared to day 1 onset and neither received antibiotic treatment (Figure S4 in [S1 File](#)).

By Day 2, after 80% of diseased animals had received antibiotic treatment, the ROC curves ([Fig 8](#), Panels D–F) reflected markedly improved classification for all three ions, with AUCs of 0.82 (0.73–0.94) for formaldehyde, 0.81 (0.73–0.92) for acetone/propanal, and 0.74 (0.60–0.88) for (C₅H₁₀O)H⁺.

While disease progression could contribute to elevated compound emissions, the data from the antibiotic trial strongly suggest that the enhanced classification performance is a pharmacological effect of antibiotic exposure, rather than a biomarker response to disease status alone.

3.6. Low-cost sensors

Two key compounds identified by the PTR-TOF were formaldehyde and acetone/propanal. Each were consistently present in the breath of healthy animals and showed a marked increase in diseased animals at the earliest clinical signs. Importantly, both compounds were among the most abundant VOCs detected, with concentrations ranging from 7 to over 400 ppb. This high abundance is a significant advantage, as it places these biomarkers well within the detection range of lower-cost sensing technologies such as the RoboScientific 720 VOC array. This greatly enhances the feasibility of using such sensors for early, non-invasive on farm disease detection.

[Fig 9A](#) illustrates the time series of formaldehyde concentrations measured by the PTR-QiTOF for calf #510923. Alongside this, the peak height from sensor 17 (of 24) on the 720 array is shown. The temporal pattern from the 720 closely aligns with the breath signal detected by the PTR-QiTOF, yielding a correlation coefficient (R^2) of 0.68. An even stronger correlation ($R^2=0.76$) is observed for the desorption slope signal from the same sensor, demonstrating the capability of this specific sensor to broadly capture the dynamics of the formaldehyde signal in breath.

However, this represents the output from just one of 24 distinct sensors contained within the 720, each generating multiple output parameters per breath sample—specifically, peak height, integrated area, absorption slope, and desorption slope. To evaluate how breath profiles diverged from the healthy baseline, cosine similarity analysis was performed multiple times, each using a different subset of these parameters. Similarity was first computed using only peak height values across all sensors, then repeated using only area, absorption slope, and desorption slope, respectively. A final analysis combined all four parameters to generate a composite similarity score. This multi-parameter approach leverages the full dimensionality of the sensor array and may offer enhanced analytical performance by capturing more nuanced changes in breath chemistry than any single parameter or sensor alone.

[Fig 9B](#) presents the results of these analyses, showing the angular distance (θ , in degrees) between each diseased-day breath sample and the healthy reference profile for calf #510923. The x-axis represents Days 1–5 of the diseased period. A pronounced deviation from the healthy profile is observed on Day 1 across all parameter sets, coinciding with the onset of clinical signs. Following antibiotic administration after the Day 1 sample, a sharp reduction in angular distance is seen on Day 2, suggesting a rapid shift in the VOC profile towards the healthy baseline. This is followed by a modest increase and stabilisation from Days 3–5, potentially indicating a new post-treatment baseline. Although some caution is required when analysing results from a single animal.

While each cosine similarity analysis revealed a broadly consistent temporal trend, the greatest magnitude of change was observed in the analysis based solely on peak height data. This suggests that peak height may be particularly sensitive to disease-related shifts in VOC emissions and could serve as a key parameter for early detection.

Interestingly, while the PTR-QiTOF revealed distinct shifts in the breath volatilome following antibiotic treatment, the 720 sensor array showed a marked reduction in angular distance from the healthy baseline. This suggests that antibiotic-induced changes may either be less detectable by the sensor array or may alter the VOC profile in a way that resembles recovery, even if the underlying physiological state has not fully returned to healthy. This highlights the importance of distinguishing between genuine biological recovery and treatment-induced shifts in VOC emissions. Notably, individual sensors within the array, such as sensor #17, were able to reproduce temporal patterns closely aligned with PTR-QiTOF measurements for specific compounds like formaldehyde. However, this reflects just one of 24 sensors, and the overall array response may average out or obscure compound-specific dynamics, especially when using composite similarity metrics.

These findings, though based on a single animal, demonstrate the value of multi-parameter sensor data and suggest that low-cost sensor arrays like the 720 may offer potential for early, non-invasive disease detection in field settings.

4. Conclusions

This study demonstrates that antibiotic treatment can significantly confound breath-based disease detection in cattle by rapidly (<1 hour) altering the volatilome in ways that mimic or obscure true disease signals. Although several VOCs

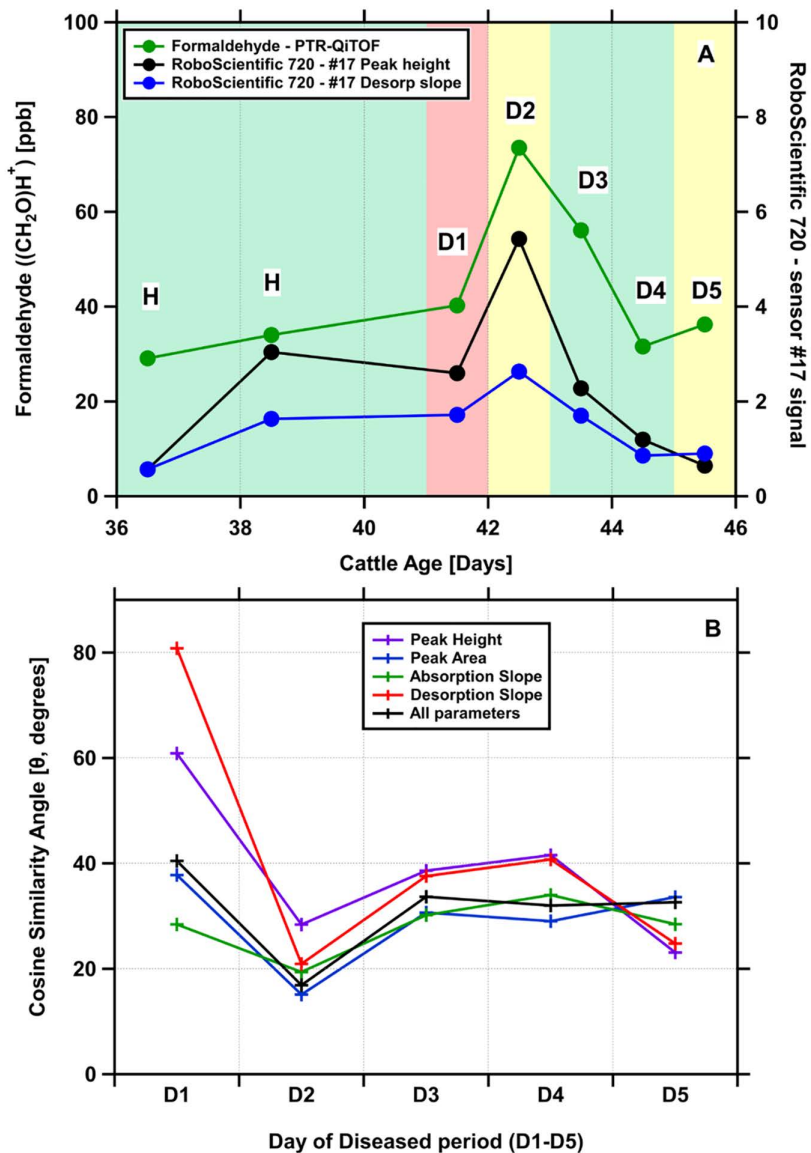


Fig 9. A. Formaldehyde concentrations in calf breath measured using PTR-QITOF, plotted against the animal's age in days. The data span the period before and during the onset of a respiratory disease episode. Also shown are the peak height and desorption slope responses from a single sensor in the RoboScientific 720 sensor array, illustrating sensor behaviour in relation to disease onset. Shaded regions represent the Modified Wisconsin Health Score: red indicates diseased (score ≥ 5), yellow indicates intermediate (score = 4), and green indicates healthy (score ≤ 3). Panel B shows the cosine similarity angle from the 720 on days 1 to 5 of the diseased period compared with the average healthy sample for this calf.

<https://doi.org/10.1371/journal.pone.0351838.g009>

increased in the days following the onset of clinical signs, only formaldehyde and acetone/propanal (and several fragment ions) were statistically elevated at the onset of clinical symptoms, prior to antibiotic administration. The strongest increases in breath markers occurred after treatment, particularly on day 2, coinciding with peak drug exposure. ROC analysis confirmed high classification performance at this time point. However, an independent trial in healthy calves showed that these discriminative patterns were largely driven by the antibiotic itself rather than the underlying pathology.

The most responsive pre-treatment compounds in diseased cattle were formaldehyde and acetone/propanal. These VOCs are among the most abundant constituents of exhaled breath, and their elevation during respiratory illness likely reflects increased oxidative stress and lipid peroxidation, processes commonly associated with inflammation and cellular damage in the lungs. Their ubiquity and biological relevance suggest that they may serve as accessible markers of host metabolic response to infection. Importantly, their high baseline abundance also offers promise for the development of low-cost, on-farm diagnostic tools, as their detection may not require the ultra-low limits of detection provided by high-end instruments such as PTR-QiTOF.

Moreover, because these compounds are consistently present in healthy animals, they provide a stable reference point for personalised monitoring, where each animal's breath profile is compared to its own healthy baseline rather than a population average. This approach may improve diagnostic sensitivity by capturing subtle, within-animal changes that would otherwise fall below population-level thresholds. For example, in this study, animals #109490 and #713323 exhibited clear increases in formaldehyde and acetone/propanal concentrations during the early stages of disease, yet these values remained below the population threshold. Such cases underscore the potential of personalised baselines to detect early physiological perturbations that might be missed by population-based screening alone.

However, it is important to acknowledge that these VOCs are not specific to BRD. Acetone, for instance, is a well-established biomarker of ketosis, and short-term reductions in feed intake during illness can induce negative energy balance and raise breath acetone independently of respiratory pathology. More broadly, both acetone and formaldehyde are associated with oxidative stress and systemic inflammation. Their elevation in breath may therefore reflect a general host metabolic response rather than a disease-specific signature. As such, while these markers show promise for detecting physiological perturbations associated with respiratory illness, their diagnostic specificity for BRD remains uncertain.

In contrast, compounds such as $(C_5H_{10}O)H^+$ and DMS showed their strongest elevations following antibiotic administration, suggesting a pharmacological rather than pathological origin. The presence of sodium formaldehyde sulfoxylate, a sulphur-containing excipient in the Alamycin formulation, further supports the hypothesis that some sulphur-containing VOCs, particularly DMS, may arise from metabolic processing of the excipient itself, rather than from the active antibiotic or disease-related pathways. Importantly, the antibiotics also amplified the very markers that initially appeared disease-associated: both formaldehyde and acetone/propanal reached their highest concentrations after treatment in both trials. This demonstrates a dual confounding effect, whereby medication elevates additional VOCs while simultaneously inflating genuine disease-linked markers.

Therefore, deviations from an animal's baseline volatilome should not be assumed to indicate disease unless potential confounders, such as recent medication or other interventions, have been ruled out, as these can generate similar shifts in VOCs. Although this analysis focused on antibiotic administration, similar confounding could occur following other interventions, including vaccinations or anti-inflammatory treatments. These findings highlight the need for caution when deploying untargeted volatilome analyses for disease diagnostics in medicated animals and suggest that future breath-based diagnostic platforms must explicitly account for pharmacological and immunological influences to avoid spurious classifications.

Importantly, the robust and consistent breath responses to oxytetracycline dihydrate (Alamycin® LA 300) observed here also point to a potential secondary application: using breath analysis to monitor treatment administration, compliance, or pharmacodynamic response in livestock. The rapid onset and reproducibility of VOC changes following injection suggest that breath profiling could offer a non-invasive means of tracking drug exposure in real time. With further development, this approach may support precision dosing strategies, reduce unnecessary antibiotic use, and improve treatment outcomes.

Supporting information

S1 File. Additional tables (S1-S2) and figures (S1-S32).
(DOCX)

Author contributions

Conceptualization: Ben Langford, Johanna Brans, Marie Haskell, Carol-Anne Duthie.

Data curation: Ben Langford.

Formal analysis: Ben Langford.

Funding acquisition: Ben Langford, Marie Haskell, Carol-Anne Duthie.

Investigation: Ben Langford, Johanna Brans, Claire Broadbent, Tim Gibson, Laura Nicoll.

Methodology: Ben Langford, Mark Hanlon, Marie Haskell, Neil J. Mullinger, Carol-Anne Duthie.

Writing – original draft: Ben Langford, Marie Haskell, Carol-Anne Duthie.

Writing – review & editing: Ben Langford, Johanna Brans, Claire Broadbent, Tim Gibson, Mark Hanlon, Marie Haskell, Laura Nicoll, Neil J. Mullinger, Carol-Anne Duthie.

References

1. Ibrahim W, Carr L, Cordell R, Wilde MJ, Salman D, Monks PS, et al. Breathomics for the clinician: the use of volatile organic compounds in respiratory diseases. *Thorax*. 2021;76(5):514–21. <https://doi.org/10.1136/thoraxjnl-2020-215667> PMID: [33414240](https://pubmed.ncbi.nlm.nih.gov/33414240/)
2. van der Schee MP, Paff T, Brinkman P, van Aalderen WMC, Haarman EG, Sterk PJ. Breathomics in Lung Disease. *Chest*. 2015;147(1):224–31.
3. Ghosh C, Leon A, Koshy S, Aloum O, Al-Jabawi Y, Ismail N, et al. Breath-Based Diagnosis of Infectious Diseases: A Review of the Current Landscape. *Clin Lab Med*. 2021;41(2):185–202. <https://doi.org/10.1016/j.cll.2021.03.002> PMID: [34020759](https://pubmed.ncbi.nlm.nih.gov/34020759/)
4. Li W, Liu Y, Lu X, Huang Y, Liu Y, Cheng S, et al. A cross-sectional study of breath acetone based on diabetic metabolic disorders. *J Breath Res*. 2015;9(1):016005. <https://doi.org/10.1088/1752-7155/9/1/016005> PMID: [25719511](https://pubmed.ncbi.nlm.nih.gov/25719511/)
5. Krilaviciute A, Heiss JA, Leja M, Kupcinskas J, Haick H, Brenner H. Detection of cancer through exhaled breath: a systematic review. *Oncotarget*. 2015;6(36):38643–57. <https://doi.org/10.18632/oncotarget.5938> PMID: [26440312](https://pubmed.ncbi.nlm.nih.gov/26440312/)
6. Wyse CA, Preston T, Yam PS, Sutton DGM, Christley RM, Hotchkiss JW, et al. Current and future uses of breath analysis as a diagnostic tool. *Vet Rec*. 2004;154(12):353–60. <https://doi.org/10.1136/vr.154.12.353> PMID: [15074325](https://pubmed.ncbi.nlm.nih.gov/15074325/)
7. Haddadi S, Koziel JA, Engelken TJ. Analytical approaches for detection of breath VOC biomarkers of cattle diseases -A review. *Anal Chim Acta*. 2022;1206:339565. <https://doi.org/10.1016/j.aca.2022.339565> PMID: [35473862](https://pubmed.ncbi.nlm.nih.gov/35473862/)
8. Weber M, Gierschner P, Klassen A, Kasbohm E, Schubert JK, Miekisch W, et al. Detection of Paratuberculosis in Dairy Herds by Analyzing the Scent of Feces, Alveolar Gas, and Stable Air. *Molecules*. 2021;26(10):2854. <https://doi.org/10.3390/molecules26102854> PMID: [34064882](https://pubmed.ncbi.nlm.nih.gov/34064882/)
9. Dobbelaar P, Mottram T, Nyabadza C, Hobbs P, Elliott-Martin RJ, Schukken YH. Detection of ketosis in dairy cows by analysis of exhaled breath. *Vet Q*. 1996;18(4):151–2. <https://doi.org/10.1080/01652176.1996.9694638> PMID: [8972064](https://pubmed.ncbi.nlm.nih.gov/8972064/)
10. Mottram TT, Dobbelaar P, Schukken YH, Hobbs PJ, Bartlett PN. An experiment to determine the feasibility of automatically detecting hyperketonaemia in dairy cows. *Livestock Production Science*. 1999;61(1):7–11. [https://doi.org/10.1016/s0301-6226\(99\)00045-7](https://doi.org/10.1016/s0301-6226(99)00045-7)
11. Darlington B. Agscent cow breath sampling: pregnancy diagnosis proof of concept. *Meat & Livestock Australia*. 2021.
12. Mortazavi S, Makouei S, Abbasian K, Danishvar S. Exhaled Breath Analysis (EBA): A Comprehensive Review of Non-Invasive Diagnostic Techniques for Disease Detection. *Photonics*. 2025;12(9):848. <https://doi.org/10.3390/photonics12090848>
13. Wang R, Davis MD. A Concise Review of Exhaled Breath Testing for Respiratory Clinicians and Researchers. *Respir Care*. 2024;69(5):613–20. <https://doi.org/10.4187/respcare.11651> PMID: [38199760](https://pubmed.ncbi.nlm.nih.gov/38199760/)
14. Bajo-Fernández M, Souza-Silva ÉA, Barbas C, Rey-Stolle MF, García A. GC-MS-based metabolomics of volatile organic compounds in exhaled breath: applications in health and disease. A review. *Front Mol Biosci*. 2024;10:1295955. <https://doi.org/10.3389/fmolb.2023.1295955> PMID: [38298553](https://pubmed.ncbi.nlm.nih.gov/38298553/)
15. Taha BA, Addie AJ, Haider AJ, Arsad N. Nanosensors Based on Breathomics for Human Disease Diagnosis: a New Frontier in Personalized Healthcare. *BioNanoSci*. 2025;15(2). <https://doi.org/10.1007/s12668-025-01876-9>
16. O'Donoghue S. A comprehensive review: Bovine respiratory disease, current insights into epidemiology, diagnostic challenges, and vaccination. *Vet Sci*. 2025;12(8):778.
17. Lindley G, Blackie N, Wathes DC, Booth RE. Development and Progression of Bovine Respiratory Disease Measured Using Clinical Respiratory Scoring and Thoracic Ultrasonography in Preweaned Calves on Dairy Farms in the United Kingdom: A Prospective Cohort Study. *Animals (Basel)*. 2025;15(3):360. <https://doi.org/10.3390/ani15030360> PMID: [39943130](https://pubmed.ncbi.nlm.nih.gov/39943130/)
18. Gaudino M, Nagamine B, Ducatez MF, Meyer G. Understanding the mechanisms of viral and bacterial coinfections in bovine respiratory disease: a comprehensive literature review of experimental evidence. *Vet Res*. 2022;53(1):70. <https://doi.org/10.1186/s13567-022-01086-1> PMID: [36068558](https://pubmed.ncbi.nlm.nih.gov/36068558/)

19. Delabougli A, James A, Valarcher J-F, Hagglund S, Raboisson D, Rushton J. Linking disease epidemiology and livestock productivity: The case of bovine respiratory disease in France. *PLoS One*. 2017;12(12):e0189090. <https://doi.org/10.1371/journal.pone.0189090> PMID: [29206855](https://pubmed.ncbi.nlm.nih.gov/29206855/)
20. Dubrovsky SA, Van Eenennaam AL, Aly SS, Karle BM, Rossitto PV, Overton MW, et al. Preweaning cost of bovine respiratory disease (BRD) and cost-benefit of implementation of preventative measures in calves on California dairies: The BRD 10K study. *J Dairy Sci*. 2020;103(2):1583–97. <https://doi.org/10.3168/jds.2018-15501> PMID: [31759608](https://pubmed.ncbi.nlm.nih.gov/31759608/)
21. Bushby EV, Thomas M, Vázquez-Diosdado JA, Occhiuto F, Kaler J. Early detection of bovine respiratory disease in pre-weaned dairy calves using sensor based feeding, movement, and social behavioural data. *Sci Rep*. 2024;14(1):9737. <https://doi.org/10.1038/s41598-024-58206-4> PMID: [38679647](https://pubmed.ncbi.nlm.nih.gov/38679647/)
22. Buczinski S, Achard D, Timsit E. Effects of calfhood respiratory disease on health and performance of dairy cattle: A systematic review and meta-analysis. *J Dairy Sci*. 2021;104(7):8214–27. <https://doi.org/10.3168/jds.2020-19941> PMID: [33896639](https://pubmed.ncbi.nlm.nih.gov/33896639/)
23. Dubrovsky SA, Van Eenennaam AL, Karle BM, Rossitto PV, Lehenbauer TW, Aly SS. Bovine respiratory disease (BRD) cause-specific and overall mortality in preweaned calves on California dairies: The BRD 10K study. *J Dairy Sci*. 2019;102(8):7320–8. <https://doi.org/10.3168/jds.2018-15463> PMID: [31202642](https://pubmed.ncbi.nlm.nih.gov/31202642/)
24. Peled N, Ionescu R, Nol P, Barash O, McCollum M, VerCauteren K, et al. Detection of volatile organic compounds in cattle naturally infected with *Mycobacterium bovis*. *Sensors and Actuators B: Chemical*. 2012;171–172:588–94. <https://doi.org/10.1016/j.snb.2012.05.038>
25. Langford B, Cash JM, Beel G, Di Marco C, Duthie C-A, Haskell M, et al. Passive breath monitoring of livestock: using factor analysis to deconvolve the cattle shed. *J Breath Res*. 2022;16(2):10.1088/1752-7163/ac4d08. <https://doi.org/10.1088/1752-7163/ac4d08> PMID: [35045410](https://pubmed.ncbi.nlm.nih.gov/35045410/)
26. Juge AE, Hall NJ, Richeson JT, Daigle CL. Using Canine Olfaction to Detect Bovine Respiratory Disease: A Pilot Study. *Front Vet Sci*. 2022;9:902151. <https://doi.org/10.3389/fvets.2022.902151> PMID: [35847637](https://pubmed.ncbi.nlm.nih.gov/35847637/)
27. Kuchmenko T, Shuba A, Umarmkhanov R, Chernitskiy A. Portable Electronic Nose for Analyzing the Smell of Nasal Secretions in Calves: Toward Noninvasive Diagnosis of Infectious Bronchopneumonia. *Vet Sci*. 2021;8(5):74. <https://doi.org/10.3390/vetsci8050074> PMID: [33925674](https://pubmed.ncbi.nlm.nih.gov/33925674/)
28. Schelkopf CS, Weaver LF, Apley MD, Pogranichniy RM, Noll LW, Bai J. Cyranose® 320 eNose effectively differentiates pre- and post-challenge respiratory samples in an induced bovine respiratory disease model. *Vet Sci*. 2025;12(6):578.
29. Masebo NT, Marliani G, Shannon Del Re F, Abram L, Cavallini D, Di Pietro M, et al. Evaluation of antimicrobial and non-steroidal anti-inflammatory treatments for BRD on health and welfare in fattening bulls: a cross-sectional study. *Vet Q*. 2024;44(1):1–11. <https://doi.org/10.1080/01652176.2024.2347928> PMID: [38711265](https://pubmed.ncbi.nlm.nih.gov/38711265/)
30. Escalona J, Soto D, Oviedo V, Rivas E, Severino N, Kattan E, et al. Beta-Lactam Antibiotics Can Be Measured in the Exhaled Breath Condensate in Mechanically Ventilated Patients: A Pilot Study. *J Pers Med*. 2023;13(7):1146. <https://doi.org/10.3390/jpm13071146> PMID: [37511759](https://pubmed.ncbi.nlm.nih.gov/37511759/)
31. Sulzer P, Hartungen E, Hanel G, Feil S, Winkler K, Mutschlechner P, et al. A Proton Transfer Reaction-Quadrupole interface Time-Of-Flight Mass Spectrometer (PTR-QiTOF): High speed due to extreme sensitivity. *International Journal of Mass Spectrometry*. 2014;368:1–5. <https://doi.org/10.1016/j.ijms.2014.05.004>
32. Steinbacher M, Dommen J, Ammann C, Spirig C, Neftel A, Prevot ASH. Performance characteristics of a proton-transfer-reaction mass spectrometer (PTR-MS) derived from laboratory and field measurements. *International Journal of Mass Spectrometry*. 2004;239(2–3):117–28. <https://doi.org/10.1016/j.ijms.2004.07.015>
33. Taipale R, Ruuskanen TM, Rinne J, Kajos MK, Hakola H, Pohja T, et al. Technical Note: Quantitative long-term measurements of VOC concentrations by PTR-MS – measurement, calibration, and volume mixing ratio calculation methods. *Atmos Chem Phys*. 2008;8(22):6681–98. <https://doi.org/10.5194/acp-8-6681-2008>
34. Li M, Bekö G, Zannoni N, Pugliese G, Carrito M, Cera N, et al. Human metabolic emissions of carbon dioxide and methane and their implications for carbon emissions. *Sci Total Environ*. 2022;833:155241. <https://doi.org/10.1016/j.scitotenv.2022.155241> PMID: [35421492](https://pubmed.ncbi.nlm.nih.gov/35421492/)
35. Dißmann L, Reinhold P, Smith H-J, Amon T, Sergeeva A, Hoffmann G. Evaluation of a Respiration Rate Sensor for Recording Tidal Volume in Calves under Field Conditions. *Sensors (Basel)*. 2023;23(10):4683. <https://doi.org/10.3390/s23104683> PMID: [37430597](https://pubmed.ncbi.nlm.nih.gov/37430597/)
36. Langford B. Early-Life Respiratory Emissions of CO₂, CH₄, and N₂O in Pre-Weaned Dairy-Bred Calves. *J Sustain Agric Environ*. 2026.
37. McGuirk SM, Peek SF. Timely diagnosis of dairy calf respiratory disease using a standardized scoring system. *Anim Health Res Rev*. 2014;15(2):145–7. <https://doi.org/10.1017/S1466252314000267> PMID: [25410122](https://pubmed.ncbi.nlm.nih.gov/25410122/)